Influence of adhesion layers on optical losses in THz quantum cascade lasers

D. V. USHAKOV,[1] A. A. AFONENKO,[1] R. A. KHABIBULLIN,[2] V. I. GAVRILENKO,[3] AND A. A. DUBINOV[3,*]

[1]*Belarusian State University, 4 Nezavisimosti Avenue, Minsk, 220030, Belarus*
[2]*V.G.Mokerov Institute of Ultra-High Frequency Semiconductor Electronics RAS, 7/5 Nagornyy proezd, Moscow, 117105, Russia*
[3]*Institute for Physics of Microstructures, Russian Academy of Sciences, GSP-105, Nizhny Novgorod, 603950, Russia*
**sanya@ipmras.ru*

Abstract: For a GaAs/AlGaAs terahertz (THz) quantum cascade laser (QCL) with a double metal waveguide (DMWG) based on *Au* and *Cu* metal plates and *Ti* and *Ta* adhesion layers, the dumping parameters and THz mode loss spectra were calculated. It has been shown that to minimize losses in high-temperature DMWG QCL designs, it is advisable to use *Ti* less than 5 nm thick or *Ta* less than 10 nm thick as adhesion layers for *Au*. The use of the proposed waveguide with a thickness of 20 μm will lead to the creation of a room temperature THz QCL.

1. Introduction

Currently, QCLs are most developed and widely used among THz compact semiconductor sources needed for a fairly wide range of tasks [1, 2]. THz QCLs have made significant progress, both in their power and operating temperatures [3, 4]. The double metal waveguide (DMWG) design, in which the active region is placed between two metal layers, has proven to be effective for THz QCLs [5]. The optical confinement factor in such waveguides is Γ~1, which is significantly higher than in plasmonic waveguides (Γ~0.3), which operate effectively even for mid-IR QCLs [6]. Typically, gold (*Au*), copper (*Cu*) and, more rarely, silver (*Ag*) are used as metal contacts [7–9]. Information on THz QCL losses over a wide range of temperatures and frequencies is needed to develop more efficient QCL operating circuits and optimized THz radiation waveguide design [8–12]. For example, the use of *Cu* as DMWG plates made it possible to reduce losses and increase the maximum operating temperature of THz QCLs in pulsed mode to ~210 K, which made it possible to use only Peltier elements for cooling [13]. However, noble metals cannot be applied directly to the surfaces of semiconductors due to poor adhesion and the possibility of solid-state diffusion between the semiconductor and the noble metal during high-temperature processes. Therefore, an intermediate metal is applied, which functions as a firmly attached adhesive layer and a diffusion barrier. A typical adhesion layer for *Au* is titanium (*Ti*) and for *Cu* is tantalum (*Ta*). However, the latest records for operating temperature were set on QCLs with *Au* plates with an adhesive layer of *Ta* [3, 4]. This work examines the influence of the thickness and material of adhesion layers on the mode loss spectra of THz QCLs for the frequency range 2 - 6.5 THz at temperatures close to room temperature. The effect of waveguide thickness on losses was also calculated. These results are important for the development of room temperature QCLs and QCLs emitting at frequencies above 6 THz.

2. Resistivity and attenuation parameter of metal layers

The dielectric constant of a metal in the THz region of the spectrum is usually described in the Drude model:

$$\varepsilon = 1 - \frac{\omega_p^2}{\omega\left(\omega + i\omega_d\right)} \quad (1).$$

The value of the plasma frequency ω_p is found as:

$$\omega_p = \sqrt{\frac{ne^2}{m\varepsilon_0}} \quad (2),$$

where n is the concentration of free electrons, e is the charge of the electron, m is the effective mass of the electron and ε_0 is the dielectric constant in vacuum. The calculated values of $\hbar\omega_p$ were 9.02 eV for *Au* and 8.98 eV for *Cu*, which is in good agreement with the work [10]. Literature data on the damping frequency ω_d vary greatly [10, 14-18] and depend on the range of frequencies studied and the temperature of the metal film deposition technology. The damping frequency ω_d is directly proportional to the resistivity ρ:

$$\omega_d = \frac{ne^2\rho}{m} \quad (3).$$

Taking into account the dominant role of the phonon scattering mechanism, the temperature dependence of resistivity can be described by the simplified formula with characteristic temperature T_x. [10]:

$$\rho(T) = \rho_0 + \frac{\rho_1}{e^{T_x/T} - 1} \quad (4).$$

Calculation using formula (4) gives good agreement with experimental data [10]. Taking into account the linear relationship between resistivity and damping frequency, from formula (3) we obtain:

$$\omega_d(T) = \frac{ne^2}{m}\rho(T) = \omega_{d0} + \frac{\omega_{d1}}{e^{T_x/T} - 1} \quad (5).$$

The approximation parameters in formulas (4–5) were found based on minimizing the mean square error and are presented in Table 1.

Table 1. Parameters for calculating the dielectric constant of *Au*, *Cu*, *Ti*, *Ta*

	n, 10^{22} cm^{-3}	$\hbar\omega_p$, eV	ρ_0, μΩ·cm	ρ_1, μΩ·cm	$\hbar\omega_{d0}$, meV	$\hbar\omega_{d1}$, meV	T_x, *K*
Au	5.91	9.02	0.514	0.396	5.6	4.3	40.2
Cu	8.45	10.80	0.377	0.568	5.9	8.9	98.9
Ti	5.54	8.74	22.984	20.558	241.7	216.2	103.51
Ta	5.67	8.84	0.0548	3.270	0.56	33.6	65.19

Practically interesting (when using Peltier elements) temperature dependences of the resistivity of metal layers of *Au*, *Cu*, *Ti* and *Ta* are presented in Fig. 1a. The resistivity of *Ti* layers increases from 52.5 to 75 μOhm×cm when the temperature changes from 200 to 300 K, which is almost six times greater than that of Ta layers (8.6–13.4 μOhm×cm). As can be seen from Fig. 1b, the attenuation energy increases with increasing temperature and for the range of 200–300 K is: 25.3–36 meV (*Au*), 19.9–28.8 meV (*Cu*), 563.3–766 meV (*Ti*), 87.5–138.9 meV (*Ta*).

Using the plasma and the damping frequencies in Table 1, the dielectric constants of the *Au*, *Cu*, *Ti* and *Ta* bulk materials can be calculated using Eq. (1) at 200 K. The results are shown in Fig. 2, and reveal larger absolute values of both the real/imaginary parts of the dielectric constant in the 2-6 THz frequency range are: -1.2×10^5– -6.6×10^4/-3.6×10^5–6.7×10^4 (*Au*), -2.5×10^5– -1.2×10^5/5.9×10^5–9.2×10^4 (*Cu*), -247.7– -247.3/1.7×10^4–5.6×10^3 (*Ti*), -9.8×10^3– -9.2×10^3/1.0×10^5–3.2×10^4 (*Ta*).

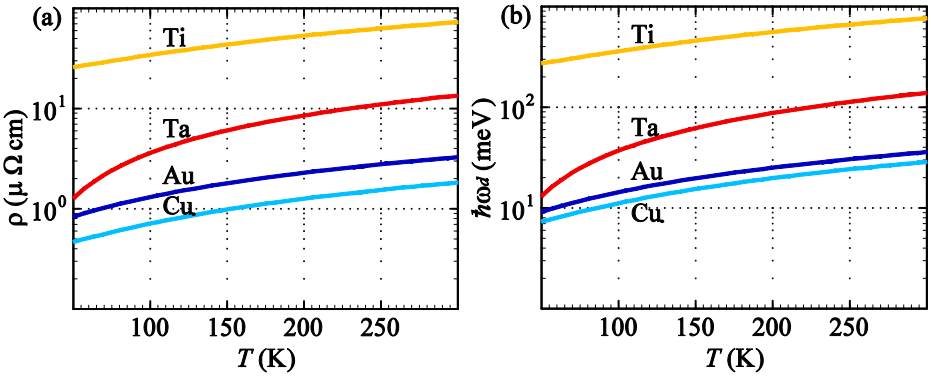

Fig. 1. Temperature dependences of resistivity ρ (a) and attenuation value $\hbar\omega_d$ (b) for various metals.

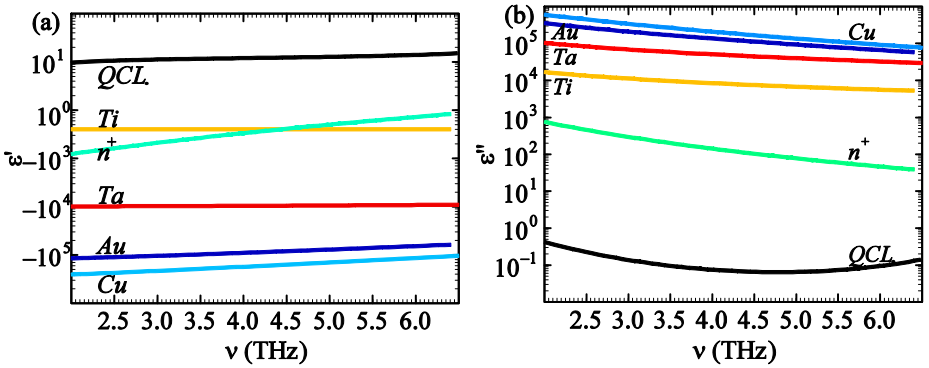

Fig. 2. Calculated real (a) and imaginary (b) parts of dielectric constants of *Au*, *Cu*, *Ti*, *Ta* films, n^+(doping 5×10^{18}cm^{-3}) and active QCL (doping 8.4×10^{15}cm^{-3}) layers at 200 K.

The active region of the QCL is sandwiched between two n^+-GaAs contact layers. The complex dielectric function of semiconductor layers was constructed as a superposition of three damped harmonic oscillators corresponding to the AC- and BC-like phonon modes for ternary alloys $A_{1-x}B_xC$ and to the free carriers, respectively. Hence [19, 20]:

$$\varepsilon(\nu) = \varepsilon_\infty \prod_{j=1}^{2} \frac{\nu^2 - \nu_{LO,j}^2 + i\nu\gamma_{LO,j}}{\nu^2 - \nu_{TO,j}^2 + i\nu\gamma_{TO,j}} - \frac{\nu_{ps}^2}{\nu(\nu + i\gamma_{ps})}, \quad (6),$$

where ε_∞, $\nu_{LO,j}$, $\nu_{TO,j}$, $\gamma_{LO,j}$, $\gamma_{TO,j}$, ν_{ps}, γ_{ps} represent, in order, the high frequency dielectric constant, the LO-,TO- phonon frequencies and the corresponding phenomenological damping parameters, semiconductor plasma frequency and the damping parameters of free carriers. The temperature dependence of the damping parameter of semiconductor layers was calculated with the help of the expression: $\gamma_{ps}(T) = e/m\mu(T)$, where $\mu(T)$ is the electron mobility as a function of temperature. The dependences of the mobility on temperature and impurity concentration for QCL layers were found on the basis of experimental data using interpolation formulas according to Ref. [21]. The values $m = 0.067$ free electron mass, μ_{QW}=10960–5634 cm^2/V·s, μ_{n+}= 2284–1617 cm^2/V·s common to both GaAs quantum wells and n^+-layers GaAs at the temperature range of 200–300 K.

The main contribution to losses of the semiconductor is given by the absorption in GaAs n^+ contact layers and $Al_{0.15}Ga_{0.85}As$/GaAs active region. The high frequency dielectric function,

GaAs- and AlAs-like mode frequencies and dumping parameters for $Al_xGa_{1-x}As$ are approximately given by Ref. [20, 22-24]. The dielectric function spectra for the n^+-GaAs contact and $Al_{0.15}Ga_{0.85}As$/GaAs active layers are also shown in Fig. 2.

3. Results of numerical calculations

Calculations of losses (α) in metal and semiconductor layers were carried out for the fundamental TM mode based on the numerical solution of the wave equation for the non-zero component of the magnetic field vector H_y, taking into account the relationship with the E_x and E_z components of the electric field, similar to the works [10, 11]:

$$\varepsilon(x)\frac{\partial}{\partial x}\frac{1}{\varepsilon(x)}\frac{\partial H_y}{\partial x}+\left(\varepsilon(x)\frac{\omega^2}{c^2}-\beta^2\right)H_y=0,\ E_x=\frac{\beta}{\varepsilon_0\varepsilon(x)\omega}H_y,\ E_z=\frac{i}{\varepsilon_0\varepsilon(x)\omega}\frac{\partial H_y}{\partial x} \quad (7),$$

where β is the longitudinal component of the mode wave vector and α = 2 Im(β). At the boundary of the layers, the continuity conditions for the tangential components of the magnetic vectors H_y and electric fields E_z are satisfied.

The configuration of the symmetrical waveguide (Fig. 3) was chosen taking into account the parameters: metal plates *Au* (*Cu*), 5–50 nm thick adhesion layers *Ti* (*Ta*), 10 μm thick GaAs/AlGaAs QCL active region. *Au*/*Cu* thickness is essentially infinite.

The results of calculating the spectra of the loss coefficient αmet on metal plates of *Au* and *Cu* for different thicknesses of *Ti* and *Ta* adhesion layers are presented in Fig. 3. As can be seen from Fig. 4, the values of the loss coefficient increase with increasing frequency and temperature. Interestingly, the *Ti*/*Au* waveguide has a weaker dependence of the loss coefficient on the thickness of the adhesion layers compared to *Ta*/*Au* and *Ta*/*Cu*. Calculations show, at a frequency of 4 THz for a temperature of 300 K for adhesion layers in the range of 5–30 nm, the losses were: 10.9–12.1 cm^{-1} (*Ti*/*Au*), 11.2–14.4 cm^{-1} (*Ta*/*Au*), 7.9–11.2 cm^{-1} (*Ta*/*Cu*). Despite the fact that the losses in *Ti* are significantly greater than in *Ta*, with the small thickness of these metals, the electric field of the mode is mainly concentrated in *Au*, so the losses in both plates are almost the same.

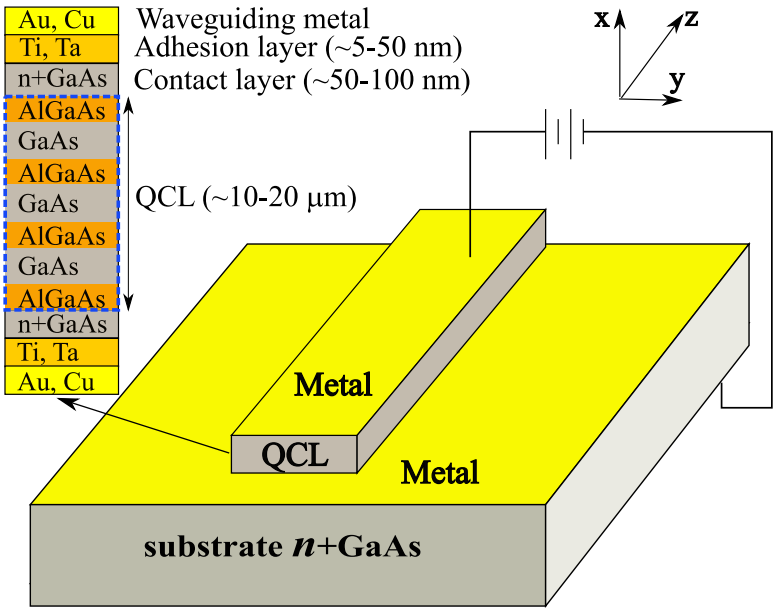

Fig. 3. Scheme of QCL waveguide

Thus, to minimize losses in high-temperature DMWG QCL designs, it is advisable to use *Ti* or *Ta* < 10 nm thick as adhesion layers for *Au*. Compared to the *Ti*/*Au* and *Ta*/*Au* waveguides, the losses in *Ta*/*Cu* waveguide is reduced by 2.6–3.3 cm^{-1} in the 3–4.7 THz range.

The total loss coefficient, including losses on the metal plates of the waveguide, resonator mirrors, absorption by optical phonons and free charge carriers, was calculated for a waveguide with both the usual thickness of 10 μm and double thickness (20 μm), which is often used to create high-power lasers [25, 26], including those operating in continuous mode, but for cryogenic temperatures. The calculations considered the QCL active region with a cascade thickness of ~55 nm. One cascade was a sequence of 4 GaAs quantum wells separated by $Al_{0.15}Ga_{0.85}As$ barrier layers with an average concentration of 8.4×10^{15} cm^{-3} or a layer concentration of 4.6×10^{10} cm^{-2}. The active region is enclosed between 50 nm thick n^{+}-GaAs contact layers with a dopant concentration 5×10^{18} cm^{-3}.

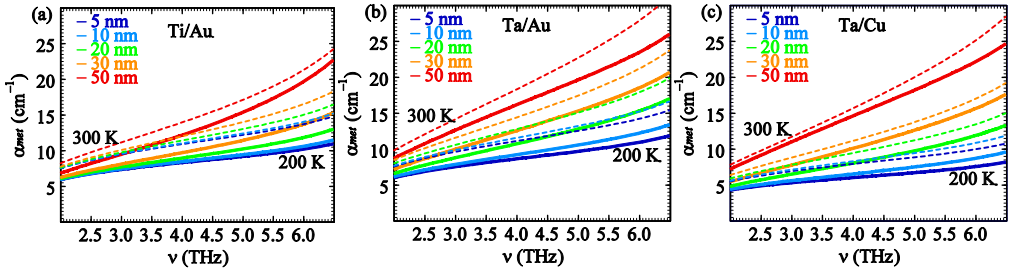

Fig. 4. Loss spectra in metal plates *Ti*/*Au* (a), *Ta*/*Au* (b) and *Ta*/*Cu* (c) for different thicknesses of *Ti* and *Ta* adhesion layers (numbers in nm to the right of the curves) at temperatures of 200 K (solid curves) and 300 K (dashed curves).

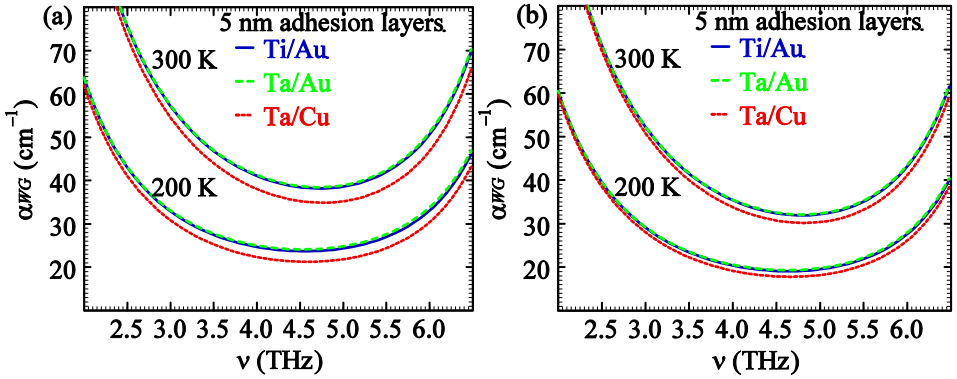

Fig. 5. Spectra of total losses in metal plates *Ti* (5 nm)/*Au*, *Ta* (5 nm)/*Au* and *Ta* (5 nm)/*Cu* for active region thicknesses of 10 μm (a) and 20 μm (b) at temperatures of 200 K and 300 K.

Fig. 5a shows that the minimum total losses in a waveguide with a thickness of 10 μm and adhesion layers of 5 nm increase from 23.7 cm^{-1} to 38.2 cm^{-1} for *Ti*/*Au* waveguide and from 21.2 cm^{-1} to 34.9 cm^{-1} for *Ta*/*Cu* waveguide with increasing temperature from 200 K to 300 K. The minimum is located around 4.7 THz. The use of a waveguide with a thickness of 20 μm (Fig. 5b) significantly reduces the minimum total losses to 18 cm^{-1} at temperature of 200 K and to 30 cm^{-1} at temperature of 300 K, which are practically independent of the selected combination of metals.

4. Conclusion

The paper calculates losses in a double metal waveguide, which is used for high-temperature terahertz QCLs. A comparison was made of losses depending on the composition of the metal plates, the thickness of the metal adhesion layer and waveguide thickness. It has been shown that minimal losses (around 30 cm^{-1}) at room temperature are achieved at a frequency of 4.7 THz in a 20 μm thick waveguide and using a 5 nm thick *Ti* or *Ta* adhesion layer. The importance of this result is that the use of recently proposed active media designs for terahertz QCLs [27, 28] for such a waveguide will lead to the creation of a THz QCL operating at room temperature. In addition, the results of the calculations show that the total losses of the considered waveguide in the frequency range 6 - 6.5 THz are less than those at frequencies below 2.5 THz. Note that QCLs in the range of 1-2.5 THz were created earlier [6], from which we can conclude that it is fundamentally possible to create currently non-existent QCLs emitting at frequencies above 6 THz [29, 30].

Funding. Russian Science Foundation (23-19-00436).

Disclosures. The authors declare no conflicts of interest.

Data availability. Data underlying the results presented in this paper are not publicly available at this time but may be obtained from the authors upon reasonable request.

References

1. A. Leitenstorfer, A. S. Moskalenko, T. Kampfrath, *et al*., "The 2023 terahertz science and technology roadmap," J. Phys. D: Appl. Phys. **56**, 223001 (2023).
2. L. Gao, C. Feng, and X. Zhao. "Recent developments in terahertz quantum cascade lasers for practical applications," Nanotechnol. Rev. **12**, 20230115 (2023).
3. A. Khalatpour, A. K. Paulsen, C. Deimert, *et al*. "High-power portable terahertz laser systems," Nat. Photon. **15**, 16–20 (2021).
4. A. Khalatpour, M. C. Tam, S. J. Addamane, *et al*. "Enhanced operating temperature in terahertz quantum cascade lasers based on direct phonon depopulation," Appl. Phys. Lett. **122**, 161101 (2023).
5. K. Unterrainer, R. Colombelli, C. Gmachl, *et al*. "Quantum cascade lasers with double metal-semiconductor waveguide resonators," Appl. Phys. Lett. **80**, 3060–3062 (2002).
6. M. S. Vitiello, G. Scalari, B. Williams, P. D. Natale, "Quantum cascade lasers: 20 years of challenges," Opt. Express, **23**(4), 5167–5182 (2015).
7. M. A. Belkin, J. A. Fan, S. Hormoz, *et al*. "Terahertz quantum cascade lasers with copper metal-metal waveguides operating up to 178 K," Opt. Express **16**(5), 3242–3248 (2008).
8. S. Fathololoumi, E. Dupont, S. G. Razavipour, *et al*. "On metal contacts of terahertz quantum cascade lasers with a metal-metal waveguide," Semicond. Sci. Technol. **26**, 105021 (2011).
9. Y. J. Han, L. H. Li, J. Zhu, *et al*. "Silver-based surface plasmon waveguide for terahertz quantum cascade lasers," Opt. Express **26**, 3814–3827 (2018).
10. D. V. Ushakov, A. A. Afonenko, A. A. Dubinov, *et al*. "Mode loss spectra in THz quantum-cascade lasers with gold- and silver-based double metal waveguides," Quant. Electron. **48**(11), 1005–1008 (2018).
11. R. Khabibullin, D. Ushakov, A. Afonenko, *et al*. "Spectra of mode loss in THz quantum cascade laser with double metal waveguide based on Au, Cu and Ag," Proc. SPIE. **11066**, 1106613 (2019).
12. M. Szyma´nski, A. Szerling, K. Kosie. "Theoretical investigation of metal–metal waveguides for terahertz quantum-cascade lasers," Opt. Quant. Electron. **47**, 843–849 (2015).
13. L. Bosco, M. Franckie, G. Scalari, *et al*. "Thermoelectrically cooled THz quantum cascade laser operating up to 210 K," Appl. Phys. Lett. **115**, 010601 (2019).
14. M. A. Ordal, L. L. Long, R. J. Bell *et al*. "Optical properties of the metals Al, Co, Cu, Au, Fe, Pb, Ni, Pd, Pt, Ag, Ti, and W in the infrared and far infrared," Appl. Opt. **22**(7), 1099–1119 (1983).
15. S. Babar and J. H. Weaver. "Optical constants of Cu, Ag, and Au revisited," Appl. Opt. **54**, 477–481 (2015).
16. L. Hall. "Survey of electrical resistivity measurements on 16 pure metals in the temperature range 0 to 273 K," National Institute of Standards and Technology, Gaithersburg, MD, 1968, [online], https://doi.org/10.6028/NBS.TN.365
17. R. A. Matula. "Electrical resistivity of copper, gold, palladium, and silver," J. Phys. Chem. Ref. Data. **8**(4), 1147–1298 (1979).
18. W. R. G. Kemp, P. G. Klemens, G. K. White. "Thermal and Electrical Conductivities of Iron, Nickel, Titanium and Zirconium at Low Temperatures," Australian J. Phys. **9**, 180–189 (1956).
19. T. Hofmann, G. Leibiger, V. Gottschalch, *et al*. "Infrared dielectric function and phonon modes of highly disordered $(Al_xGa_{1-x})_{0.52}In_{0.48}P$," Phys. Rev. B **64**, 155206 (2001).
20. D. J. Lockwood, G. Yu, N. L. Rowell. "Optical phonon frequencies and damping in AlAs, GaP, GaAs, InP, InAs and InSb studied by oblique incidence infrared spectroscopy," Solid State Commun. **136**, 404–409 (2005).
21. V. Palankovski and R. Quay, *Computational Microelectronics* (Springer, New York, 2004).

22. S. Adachi. “GaAs, AlAs, and $Al_xGa_{1-x}As$: Material parameters for use in research and device applications,” J. Appl. Phys. **58**, R1–R29 (1985).
23. O. K. Kim, W. G. Spitzer. “Infrared reflectivity spectra and Raman spectra of $Ga_{1-x}Al_xAs$ mixed crystals,” J. Appl. Phys. **50**, 4362–4370 (1979).
24. G. Irmer, M. Wenzel, J. Monecke. “The temperature dependence of the LO(T) and TO(T) phonons in GaAs and InP,” Phys. Stat. Solidi (b) 195, 85–95 (1996).
25. L. H. Li, L. Chen, J. R. Freeman, *et al*. “Multi-Watt high-power THz frequency quantum cascade lasers,” Electron. Lett., **53**(12), 799–800 (2017).
26. C. Song, M. Salih, L. H. Li, *et al*. “High-power density, single plasmon, terahertz quantum cascade lasers via transverse mode control,” Appl. Phys. Lett. **122**, 121108 (2023).
27. V. Rindert, E. Önder, and A. Wacker. “Analysis of High-Performing Terahertz Quantum Cascade Lasers,” Phys. Rev. Appl. **18**, L041001 (2022).
28. B. Wen and D. Ban. “Theoretical Study of Quasi One-Well Terahertz Quantum Cascade Laser,” Photonics, **9**, 247 (2022).
29. D. V. Ushakov, A. A. Afonenko, An. A. Afonenko, *et al*. “Feasibility of GaAs/AlGaAs quantum cascade laser operating above 6 THz,” J. Appl. Phys. **135** (13), 133108 (2024).
30. D. V. Ushakov, A. A. Afonenko, R. A. Khabibullin, *et al*. “Phosphides-based terahertz quantum-cascade laser,” Phys. Stat. Solidi RRL, **18**, 2300392 (2024).